MCL-1 is essential for survival but dispensable for metabolic fitness of FOXP3^{+} regulatory T cells

Charis E Teh[1,2,*], Alissa K Robbins[1,2,*], Darren C Henstridge[3,6], Grant Dewson[1,2], Sarah Diepstraten[1,2], Gemma Kelly[1,2], Mark A Febbraio[3,7], Sarah S Gabriel[4,5], Lorraine A O'Reilly[1,2], Andreas Strasser[1,2] and Daniel HD Gray[1,2]

[1] The Walter and Eliza Hall Institute of Medical Research, 1G Royal Parade, Parkville, VIC, Australia

[2] Department of Medical Biology, The University of Melbourne, Parkville, VIC 3052, Australia

[3] Cellular and Molecular Metabolism Laboratory, Baker Heart and Diabetes Institute, Melbourne, Victoria, Australia

[4] The Peter Doherty Institute for Infection and Immunity, Melbourne, Victoria, Australia

[5] Department of Microbiology and Immunology, The University of Melbourne, Parkville, Victoria, Australia

[6] Current Address: School of Health Sciences, University of Tasmania, Launceston, Tasmania, Australia

[7] Current Address: Drug Discovery Biology, Monash Institute of Pharmaceutical Sciences, Melbourne, Victoria, Australia

[*] These authors contributed equally to this work

Correspondence should be addressed to DHDG

E-mail: dgray@wehi.edu.au

Telephone: +613 93452930

Fax: +613 93470852

ABSTRACT

FOXP3$^+$ regulatory T (Treg) cells are essential for maintaining immunological tolerance. Given their importance in immune-related diseases, cancer and obesity, there is increasing interest in targeting the Treg cell compartment therapeutically. New pharmacological inhibitors that specifically target the pro-survival protein MCL-1 may provide this opportunity, as Treg cells are particularly reliant upon this protein. However, there are two distinct isoforms of MCL-1; one located at the outer mitochondrial membrane (OMM) that is required to antagonize apoptosis, and another at the inner mitochondrial membrane (IMM) that is reported to maintain IMM structure and metabolism via ATP production during oxidative phosphorylation. We set out to elucidate the relative importance of these distinct biological functions of MCL-1 in Treg cells to assess whether MCL-1 inhibition might impact upon the metabolism of cells able to resist apoptosis. Conditional deletion of *Mcl1* in FOXP3$^+$ Treg cells resulted in a lethal multi-organ autoimmunity due to the depletion of the Treg cell compartment. This striking phenotype was completely rescued by concomitant deletion of the apoptotic effector proteins BAK and BAX, indicating that apoptosis plays a pivotal role in the homeostasis of Treg cells. By contrast, MCL-1-deficient Treg cells rescued from apoptosis displayed normal metabolic capacity. Moreover, pharmacological inhibition of MCL-1 in Treg cells resistant to apoptosis did not perturb their ~~mitochondrial membrane potential or~~ metabolic function. We conclude that Treg cells require MCL-1 only to antagonize apoptosis and not for metabolism. Therefore, MCL-1 inhibition could be used to manipulate Treg cell survival for clinical benefit without effecting the metabolic fitness of cells resisting apoptosis.

INTRODUCTION

Apoptosis is an evolutionally conserved cell death mechanism essential for development, homeostasis and tumour suppression. Apoptosis can be triggered through the B cell lymphoma 2 (BCL-2)-regulated (or intrinsic or mitochondrial) pathway [1]. The pathway is regulated by members of the BCL-2 family of proteins in activities that converge on the mitochondrial outer membrane. During apoptosis, the effector proteins, BAK and/or BAX become activated, changing conformation to permeabilize the outer mitochondrial membrane (OMM) [2]. Mitochondrial proteins, such as cytochrome c and SMAC/DIABLO, then leak out of the mitochondria and initiate a caspase activation cascade to mediate cell demolition [3]. Therefore, the activation of BAX and/or BAK represents the fulcrum of the BCL-2-regulated pathway of apoptosis. In healthy cells, pro-survival proteins such as BCL-2, BCL-XL and MCL-1 restrain BAX and BAK to prevent apoptosis. Cellular stresses, such as γ-irradiation, growth factor deprivation or hypoxia induce activation or upregulation of the pro-apoptotic BH3-only members of the BCL-2 family, such as BIM, PUMA or NOXA [4]. The BH3-only proteins can interact with the pro-survival BCL-2 family members to relieve their inhibition of BAX and BAK, and can also directly activate these effector proteins to induce apoptosis [5]. Different cell types have different expression profiles of the various BCL-2 family proteins and the cellular response to different cytotoxic stimuli can therefore vary. For example, platelets are particularly reliant upon BCL-XL for their survival, whereas many lymphocyte subsets are dependent upon MCL-1, and to a lesser extent, upon BCL-2 or BCL-XL [6].

Regulatory T (Treg) cells are a subset of $CD4^+$ T cells essential for maintaining immunological tolerance by constraining the activation, proliferation and cytokine production of $CD4^+$ and $CD8^+$ T cells [7]. Treg cells are characterised by expression of the

transcription factor forkhead box P3 (FOXP3) [8], which drives the unique transcriptional signature of this cell population, and also by high levels of IL-2 receptor (IL-2R or CD25) on the cell surface [9]. These high levels of IL-2R play a key role in the unique homeostatic properties of Treg cells [10], and also contribute to their suppressive function through outcompeting conventional T cells for available IL-2. The importance of Treg cells in maintaining immune homeostasis is underscored by the fatal autoimmune phenotype that results from the disruption of *FoxP3* in mice and humans [8, 11, 12, 13, 14, 15]. Of note, Treg cells have also been implicated in a wide variety of other diseases [16] and there is increasing interest in targeting the Treg cell compartment therapeutically to augment immune responses in diseases, such as chronic infections, cancer and obesity induced metabolic disease [17 18, 19, 20, 21].

Treg cell survival and homeostasis relies upon the pro-survival protein MCL-1 [22]. Although many other immune cell types require a basal level of MCL-1 expression for their survival [23], Treg cells express relatively higher amounts of MCL-1 than other T cell subsets [22], in part controlled by IL-2R signalling [10, 22]. The first MCL-1 inhibitor, S63845, showed promising results in many pre-clinical models of human cancers [24, 25, 26] and was assessed to be safe and tolerable in a mouse model of humanised *Mcl-1* [27]. Recently, clinical trials have commenced for several MCL-1 inhibitors, including S64315/MIK665 (a derivative of S63845[24]), AMG 176 and AMG 397 (NCT0299248, NCT02675452 and NCT03465540, respectively) in cancer [28]. An important consideration in the deployment of MCL-1 inhibitors in the clinic is their potential to inhibit the two distinct isoforms and functions of MCL-1. One isoform is located at the outer mitochondrial membrane (OMM) and restrains BAX plus BAK and is thus required to inhibit apoptosis. The other MCL-1 isoform is located at the inner mitochondrial membrane (IMM) and is essential for IMM structure and plays a role in

metabolism by impacting ATP production during oxidative phosphorylation [29, 30]. Treg cells from mice express both of these isoforms [22]. Although inhibiting the pro-survival form of MCL-1 at the OMM is desirable for killing cancer cells, there is evidence that the MCL-1 inhibitors, MIM-1 and S63845 can also disrupt the IMM form of MCL-1 in human stem cells [31]. Hence, as MCL-1 inhibitors progress in clinical development, it will be imperative to dissect the relative importance of the two major functions of MCL-1 in key cell types, such as lymphocytes, to understand the potential impacts of MCL-1 inhibition and indications beyond directly targeting cancer cells.

Here, we study MCL-1 function in Treg cells because they are highly reliant upon MCL-1 and impaired survival or metabolic function in Treg cells induces clear, fatal immune outcomes *in vivo* [22, 33]. MCL-1-deficiency in Treg cells resulted in fatal multi-organ immune pathology, resembling that observed in the *Foxp3*-deficient *scurfy* mutant mouse. This phenotype could be completely rescued by the genetic deletion of pro-apoptotic *Bak* and *Bax*, indicating that only the pro-survival function of MCL-1 is essential for Treg cell homeostasis and immune tolerance. MCL-1-deficient Treg cells rescued from apoptosis also had normal metabolic capacity. Furthermore, we demonstrate that the inhibition of MCL-1 with S63845 did not perturb the metabolic function of Treg cells rendered refractory to apoptosis. These data suggest that MCL-1 inhibition could be used to manipulate Treg cell survival for clinical benefit, without impacting the metabolic fitness of the remaining Treg cells or potentially other lymphocytes.

RESULTS

Loss of MCL-1 in Treg cells drives a fatal multi-organ autoimmunity that is rescued by BAK deficiency

To determine the impact of MCL-1 loss on Treg cell homeostasis, we inter-crossed mice with floxed *Mcl1* alleles (*Mcl1*$^{fl/fl}$ mice) [34] with another strain expressing the Cre-recombinase and a YFP reporter under the control of the Treg-specific gene, *Foxp3,* (*FoxP3*$^{Cre\text{-}IRES\text{-}YFP}$ mice) [35]. This inter-cross generated mice with Treg cell-specific deletion of *Mcl1* (hereafter referred to as *Mcl1*$^{\Delta FoxP3}$ mice). We confirmed MCL-1-deficiency was specific to FOXP3^{+} cells by assaying the amount of MCL-1 protein by intracellular flow cytometry in CD4^{+} FOXP3^{-} T and CD4^{+} FOXP3^{+} Treg cells (**Figure 1A**). Accordingly, we observed a significantly lower fluorescence intensity of MCL-1 specifically in the Treg cell population compared to CD4^{+} FOXP3^{-} T cells (**Figure 1B**) or Treg cells from MCL-1-sufficient mice (not shown). Consistent with previous findings [22], MCL-1-deficiency in Treg cells led to the development of a lethal lympho-infiltrative disease, with a median survival age of 76 days (**Figure 1C**). The auto-inflammatory phenotype observed in *Mcl1*$^{\Delta FoxP3}$ mice resembled that observed in *scurfy* mice [36, 37], albeit with a slightly slower kinetics (**Figure 1C**). There was significant elevation of IgE in the sera of *Mcl1*$^{\Delta FoxP3}$ compared to wild-type (WT) mice (**Figure 1D**) and histological analysis revealed severe lymphocytic infiltration of a range of peripheral organs, including the lung, pancreas and salivary glands (**Figure 1E and F**); all hallmarks of the multi-organ autoimmunity accompanying Treg cell deficiency consistent with the early lethality in *Mcl1*$^{\Delta FoxP3}$ mice.

To test whether abrogation of the BCL-2-regulated pathway of apoptosis was sufficient to prevent disease in *Mcl1*$^{\Delta FoxP3}$ mice, they were inter-crossed with *Bax*$^{fl/fl}$ *Bak*$^{-/-}$ [38] mice to create *Mcl1*$^{\Delta FoxP3}$ *Bax*$^{\Delta FoxP3}$ *Bak*$^{-/-}$ animals. These mice survived to 125 days without any overt signs of pathology (**Figure 1C**). In addition, serum IgE and all histological parameters in these *Mcl1*$^{\Delta FoxP3}$ *Bax*$^{\Delta FoxP3}$ *Bak*$^{-/-}$ mice were comparable to wild-type counterparts (**Figure 1D-F**). Three additional *Mcl1*$^{\Delta FoxP3}$ *Bax*$^{\Delta FoxP3}$ *Bak*$^{-/-}$ mice were aged to 228 days and also survived free

of disease. Interestingly, the loss of BAK alone was sufficient to rescue lethal auto-inflammation in *Mcl1*$^{\Delta FoxP3}$ mice (**Figure 1C**), consistent with the predilection for MCL-1 to interact with this apoptotic effector compared to BAX [39, 40]. These results indicate that impairing BAK- (and to a lesser extent also BAX-) mediated apoptosis rescues the lethal autoimmunity observed in *Mcl1*$^{\Delta FoxP3}$ mice.

Deletion of BAK and BAX in *Mcl1*$^{\Delta FoxP3}$ mice is sufficient to restore Treg cells and immune tolerance

BAK and BAX are essential for execution of the intrinsic pathway of apoptosis but are dispensable for the metabolic function of MCL-1. Therefore, we next assessed how concomitant loss of BAK and BAX prevented disease in *Mcl1*$^{\Delta FoxP3}$ mice and whether Treg cells rescued by prevention of apoptosis exhibited signs of perturbed differentiation or phenotype suggestive of impaired metabolism. Consistent with the kinetics of *Foxp3*^{Cre}-mediated deletion, *Mcl1*$^{\Delta FoxP3}$ mice generated normal numbers of CD4^{+}FOXP3^{+} Treg cells in the thymus (**Figure 2A, B**). As previously reported [22], *Bax*$^{\Delta FoxP3}$ *Bak*$^{-/-}$ mice have a significant proportional and numerical increase in the thymic Treg compartment compared to WT controls (**Figure 2A, B**). This increase was maintained with concomitant loss of *Mcl1* in Treg cells (**Figure 2A, B**), indicating that thymic Treg cell maturation was normal or enhanced.

Treg cells in the peripheral lymphoid organs (spleen and lymph nodes) were substantially diminished in *Mcl1*$^{\Delta FoxP3}$ mice compared to WT controls (**Figure 2C, D**), consistent with the notion that loss of this population led to loss of immune tolerance and fatal autoimmunity [22]. *Bax*$^{\Delta FoxP3}$ *Bak*$^{-/-}$ mice had a greater proportion and number of Treg cells in the periphery compared to WT controls (**Figure 2C, D**). These BAX- and BAK-deficient Treg cells had comparable suppressive capacity to Treg cells from WT controls (Supplementary Figure S1A).

The Treg population in *Mcl1*$^{\Delta FoxP3}$ *Bax*$^{\Delta FoxP3}$ *Bak*$^{-/-}$ mice was expanded to the same extent as *Bax*$^{\Delta FoxP3}$ *Bak*$^{-/-}$ controls (**Figure 2C, D**), indicating that loss of the downstream apoptotic effector proteins completely rescued the death of MCL-1-deficient Treg cells.

The activation of CD4^{+}FOXP3^{-} and CD8^{+} T cell populations inversely correlated with Treg cell numbers. *Mcl1*$^{\Delta FoxP3}$ mice had an approximately 2- to 3-fold increase in the proportion and number of activated CD44^{high}CD62L^{low} cells compared to WT mice (**Figure 3A, B**), consistent with a severe defect in immune tolerance. By contrast, CD4^{+}FOXP3^{-} and CD8^{+} cell activation in *Mcl1*$^{\Delta FoxP3}$ *Bax*$^{\Delta FoxP3}$ *Bak*$^{-/-}$ mice was comparable to WT controls (**Figure 3A, B**). These data indicate that abrogation of BAK/BAX-mediated apoptosis is sufficient to restore Treg cell homeostasis and immune tolerance in the absence of the pro-survival protein, MCL-1, at least until 228 days. Furthermore, MCL-1-deficient Treg cells are capable of suppressing the activation of autoreactive CD4^{+} and CD8^{+} cells to preserve immune tolerance.

Neither genetic deletion of *Mcl1* nor pharmacological inhibition of MCL-1 affects Treg cell metabolism

Deletion of *Mcl1* has been reported to impair the metabolic function in other cell types, such as cardiomyocytes and stem cells [29, 30, 31]. Our data indicated that *Mcl1*-deficient Treg cells rendered resistant to apoptosis had normal homeostasis and function. However, since Treg cells also express the lower molecular weight isoform of MCL-1 that localizes to the IMM [22] (as do those from *Bax*$^{\Delta FoxP3}$ *Bak*$^{-/-}$ mice, (**Supplementary Figure S1B**)), it was important to directly test their metabolic capacity. Quantification of mitochondrial membrane potential, using Mitotracker Orange staining, in Treg cells from WT, *Bax*$^{\Delta FoxP3}$ *Bak*$^{-/-}$ and *Mcl1*$^{\Delta FoxP3}$ *Bax*$^{\Delta FoxP3}$ *Bak*$^{-/-}$ mice was performed (the paucity of Treg cells in *Mcl1*$^{\Delta FoxP3}$ mice precluded their analysis). ~~Consistent with a previous report, wWe~~ We observed somewhat reduced

mitochondrial membrane potential in Treg cells lacking BAX and BAK compared to WT cells (**Figure 4A**). However, compared to *Bax*$^{\Delta FoxP3}$ *Bak*$^{-/-}$ controls, MCL-1 deficient Treg cells did not show substantial changes in oxidative membrane potential, indicating that overall mitochondrial membrane potential was comparable (**Figure 4A**).

For a more detailed analysis of Treg cell metabolic capacity, these cells were purified from *Bax*$^{\Delta FoxP3}$ *Bak*$^{-/-}$ and *Mcl1*$^{\Delta FoxP3}$ *Bax*$^{\Delta FoxP3}$ *Bak*$^{-/-}$ mice and analysed on the Seahorse XF platform to detect changes in respiration in MCL-1-deficient Treg cells. Since the numbers of Treg cells that can be recovered from mice was limiting, we performed three independent experiments each with technical replicates of 600,000 cells pooled from *n*=2-5 mice. Representative data from one experiment are shown in Figure 4B-D and the other replicates presented in Supplementary Figure S2. Despite the reduction in mitochondrial membrane potential detected with Mitotracker staining, Treg cells from *Bax*$^{\Delta FoxP3}$ *Bak*$^{-/-}$ mice did not demonstrate gross defects in respiration compared to those from WT mice across multiple experiments (**Fig 4B, C; Supplementary Figure S2A, C**). This finding is consistent with previous data showing that BAX- and BAK-deficient MEF have normal respiratory capacity [41] and our findings that Treg cells from *Bax*$^{\Delta FoxP3}$ *Bak*$^{-/-}$ mice retain normal functional capacity (**Supplementary Figure S2A**).

As MCL-1 was reported to be required for the oligomerization of the F_1F_0-ATP Synthase complex in some cell types [29], we anticipated that Treg cells lacking MCL-1 would have impaired ATP production through mitochondrial oxidative phosphorylation. The oxygen consumption rate (OCR) is a surrogate of mitochondrial respiration. Basal respiration is calculated as the difference between non-mitochondrial oxygen consumption (i.e. the OCR following inhibition of the RC complex I and complex III with the compounds Rotenone and

Antimycin A, respectively) and the initial OCR before the addition of Oligomycin (**Figure 4B, C; Supplementary Figure S2A, C**). We found that Treg cells from *Mcl1*$^{\Delta FoxP3}$ *Bax*$^{\Delta FoxP3}$ *Bak*$^{-/-}$ mice had similar basal respiration as *Bax*$^{\Delta FoxP3}$ *Bak*$^{-/-}$ controls (**Figure 4B, C; Supplementary Figure S2A, C**). Loss of IMM MCL-1 has also been reported to reduce maximal respiration [29], which is calculated as the difference between the OCR following addition of the uncoupler FCCP, and non-mitochondrial oxygen consumption (**Figure 4B, D; Supplementary Figure S2B, D**). We observed no significant differences in maximal respiration between Treg cells from the *Mcl1*$^{\Delta FoxP3}$ *Bax*$^{\Delta FoxP3}$ *Bak*$^{-/-}$ and the control (**Figure 4B, D; Supplementary Figure S2B, D**). These data indicate that the genetic deletion of *Mcl1* does not affect the metabolic function of Treg cells when they are protected from apoptosis by the loss of BAX and BAK.

Clinical trials of the MCL-1 inhibitor, S64315/MIK665 (a derivative of S63845) have commenced. Although it has not been directly demonstrated that S63845 interacts with the IMM isoform of MCL-1, it has been published that it can disrupt interactions between MCL-1 and the matrix-localized protein, OPA-1 [9]. Therefore, we next tested whether S63845 had any direct or indirect effects on metabolism in Treg cells incapable of undergoing apoptosis due to the loss of BAX and BAK. Treg cells were harvested from haematopoietic chimeras reconstituted with bone marrow from *Bak*$^{-/-}$ mice (to obtain a sufficient number of cells) and treated with doses of S63845 that were either sub-optimal (0.1 μM) or sufficient (1 μM) for induction of apoptosis in WT Treg cells (**Supplementary Figure S3**) or a vehicle control and analysed on the Seahorse XF platform (**Figure 4E**). Treatment with S63845 had no significant impact on either basal (**Figure 4F**) or maximal (**Figure 4G**) oxygen consumption. Therefore, the data from the genetic and pharmacological inhibition collectively indicate that MCL-1 is dispensable for Treg cell metabolism.

DISCUSSION

As inhibitors of MCL-1 proceed to clinical testing, an important consideration is how these compounds might impact on the immune system. MCL-1 supports the survival of many different immune cell types but may also fulfil roles in mitochondrial dynamics and function in cells that can withstand partial MCL-1 inhibition. Treg cells are especially important in this context, given their heightened homeostatic turnover and critical role in maintaining immune tolerance. Here we report that only the anti-apoptotic function and not the metabolic function of MCL-1 is required for Treg cell homeostasis and suppression of autoimmunity. ~~Deletion of~~ MCL-1 deficiency in Treg cells resulted in a lethal autoinflammatory phenotype in mice that was wholly rescued by the concomitant deletion of the apoptotic 'effector' proteins BAK and BAX to at least 228 days of age. Furthermore, in contrast to other cell types, genetic deletion or pharmacological inhibition of MCL-1 did not alter cellular metabolism in Treg cells.

These data are in accord with previous studies showing a key role for MCL-1 in preventing BAX/BAK-mediated apoptosis in cardiomyocytes and activated T cells [30, 42]. However, although the IMM isoform of MCL-1 was reported to also have a role in cardiomyocyte metabolism [30] and in maintaining the integrity of the mitochondrial matrix in stem cells [31], our results suggest it is dispensable for these roles in Treg cells. These results would appear to be somewhat counterintuitive, as Treg cells have a greater reliance on oxidative phosphorylation for their ATP production and function than Tconv cells [43, 44]. However, another BCL-2 family member BCL-XL, has also been reported to have a similar role in mitochondrial inner matrix stabilisation and a bioenergetic role in oxidative phosphorylation [45]. It is possible that there is a cooperating or overlapping role of these proteins in cell metabolism that allows Treg cells to overcome the loss or inhibition of MCL-1. Alternatively, it may be the case that, as with cell type specific preferences for one pro-survival BCL-2 family member over others in inhibiting

apoptosis, either BCL-XL or MCL-1 may have precedence over the other in maintaining the metabolic function in different cell types. Yet another possibility is that neither MCL-1 nor BCL-XL are required to serve a role in the metabolic fitness of Treg cells. These considerations highlight the need to better understand the molecular mechanisms by which BCL-2 family members impact on mitochondrial dynamics and function.

It is important to consider that all the experiments reported here were carried out under steady state conditions. In manipulating Treg cell populations for therapeutic utility, there may be different requirements for the inner mitochondrial matrix isoform of MCL-1 in conditions where the external environment may impact Treg cell metabolism and function, such as infection states or the tumour microenvironment [46, 47]. For example, Hypoxia Inducible Factor 1 alpha (HIF-1α) and mammalian target of rapamycin complex 1 (mTORC1) are up-regulated in Treg cells in the tumor microenvironment or infection settings, respectively. Both of these can induce different metabolic states in Treg cells [33, 48, 49, 50] that may change their requirement for IMM MCL-1.

Nevertheless, our data from genetic and pharmacological models indicates that MCL-1 is not required for mitochondrial metabolism in Treg cells ~~(and probably all lymphocytes)~~ but functions only to antagonise the intrinsic pathway of apoptosis. These findings highlight context-specific requirements for MCL-1 among cell types and have bearing on the clinical use of inhibitors of MCL-1 for cancer treatment or manipulation of Treg cells in other diseases.

METHODS AND MATERIALS

Mice. *Mcl1*$^{\Delta FoxP3}$, *Bax*$^{\Delta FoxP3}$*Bak*$^{-/-}$, *Mcl1*$^{\Delta FoxP3}$*Bak*$^{-/-}$ and *Mcl1*$^{\Delta FoxP3}$*Bax*$^{\Delta FoxP3}$*Bak*$^{-/-}$ mice were generated on, or backcrossed greater than 10 times onto, the C57BL/6 background. All mice

were housed at The Walter and Eliza Hall Institute of Medical Research (WEHI) under specific pathogen-free conditions, and experiments were carried out in accordance with the Animal Ethics Committee guidelines of the Melbourne Research Directorate. For experimentation, both female and male mice were used and mice of each genotype were randomized into groups. Disease development was monitored by frequent observation and post-mortem analysis. Cohorts of mice for the survival test were removed from the study at death, when mice lost more than 10% of peak body weight or when veterinary advice indicated likely death within 48 h. The animal technicians assessing the welfare of the mice were blinded to the expected outcomes.

Flow cytometry. Single-cell suspensions of organs were stained with fluorochrome- or biotin-conjugated antibodies (produced by BioLegend except where indicated) to the following proteins: CD4 (clone GK1.5), CD8 (clone 53-6.7), CD25 (clone PC61.5), TCRβ (clone H57-597), CD44 (clone IM7), CD62L (clone MEL-14), FOXP3 (eBiosciences, clone FJK-16) and MCL-1 (Produced in house at WEHI, clone 19c4-15). Intracellular staining for FOXP3 and MCL-1 was performed after fixation and permeabilization using the eBiosciences FOXP3 staining kit. Sample data were acquired on an LSRII or Fortessa flow cytometer (BD Biosciences) and analyzed using FlowJo software (TreeStar). Mitochondrial membrane potential was assessed by labelling with 100 nM Mitotracker Orange CMTMRos for 20 min at 37°C prior to addition of surface stains.

IgE ELISA. Serum IgE concentrations were determined by ELISA using sheep anti-mouse Ig antibodies (Silenus Laboratories) as a capture reagent, and developed with mouse IgE-specific goat antibodies that had been conjugated with horseradish peroxidase (Southern Biotechnology).

Histology. Tissues were fixed in formalin, embedded, sectioned, and stained with haematoxylin and eosin (H&E). Leukocyte infiltration was scored as 0, 1, 2, 3, 4 and 5 indicating none, trace, mild, moderate, severe or extremely severe lymphocytic infiltration and tissue destruction, respectively [51]. The organs analyzed included the eyes, salivary glands, testes or ovaries, stomach, intestines, pancreas, kidney, liver, and lungs. Slides were imaged under the Nikon 90i Upright/Widefield research microscope and scored by a reviewer blinded to the mouse identity and genotype.

Hematopoietic reconstitution. For generation of hematopoietic chimeras, adult C57BL/6.CD45.1 mice were irradiated with two doses of 5.5 Gy 3 h apart and reconstituted by intravenous injection of $2x10^6$ bone marrow cells. Mice received 100 μg of THY1 mAb (clone T24) by the intra-peritoneal (i.p.) route 24 h following injection of BM cells to eliminate residual donor T cells and mice were then left for 8 weeks prior to analysis.

Bioenergetic analysis. All bioenergetics and mitochondrial function analyses were performed using the Seahorse XF96 Extracellular Flux Analyser (Seahorse Bioscience). Sorted Treg cells were seeded into a CellTek (Corning) coated 96-well Seahorse plate in Seahorse XF assay media (pH 7.4; Agilent) supplemented with 5mM D-Glucose (Ajax Finechem), 1mM Sodium Pyruvate (Gibco) and 2mM L-Glutamine (Gibco) at a density of 6 x 10^5 cells/well. The OCR was measured sequentially after the addition of S63845 (Active Biochem), 1 μM oligomycin (Agilent), 1 μM FCCP (Agilent) and 0.5 μM rotenone and antimycin A (Agilent).

***In vitro* apoptosis assays.** Mouse spleen cells were cultured at 37°C in 10% CO_2 for 48 h in RPMI-1640 media supplemented with 10% Fetal Calf Serum (Sigma) in the presence of varying concentrations of S63845 (Active Biochem) or dimethyl sulfoxide (DMSO; Sigma) vehicle control. Viability was assayed using the LIVE/DEAD fixable green dead cell stain kit (Invitrogen). Treg cells were identified with fluorochrome-conjugated antibodies (produced by

BioLegend except where indicated) to the following proteins: CD4 (clone GK1.5), CD25 (clone PC61.5), CD3 (clone 17A2), and FOXP3 (eBiosciences, clone FJK-16). Intra-cellular staining for FOXP3 was performed after fixation and permeabilization using the eBiosciences FOXP3 staining kit. Sample data were acquired on a Fortessa flow cytometer (BD Biosciences) and analyzed using FlowJo software (TreeStar).

***In vitro* Treg cell suppression assays.** Splenic $CD4^+CD25^+$ Treg cells were FACS purified from WT control or *Casp8*$^{\Delta Foxp3}$ mice. $CD4^+CD25^-$ Tconv cells from WT control mice were FACS purified as responder cells and labelled with 5 μM Cell Trace Violet (Life Technology). Antigen presenting cells (APCs) were splenocytes from WT mice irradiated with 30 Gy. Responder cells (1×10^4), APCs (4×10^4), and different concentrations of Tregs (1:1-1:10 Treg:Tconv ratio, 1×10^4 – 1000 Tregs) were activated with 0.5 μg/mL anti-CD3 antibody in a 96-well round bottomed plate. Cells were acquired by BD Fortessa, and the division index of responder cells was analyzed using FlowJo based on the dilution of Cell Trace Violet.

Western Blotting. Splenic $CD4^+CD25^+YFP^+$ Treg and $CD4^+CD25^-$ YFP^- Tconv cells were sorted, washed in PBS and resuspended in reducing SDS-PAGE sample buffer. Samples were electrophoresed on a 12% Tris-glycine gel (BioRad) and transferred to a PVDF membrane (BioRad). Membranes were blocked in 5% (w/v) low fat milk in TBS-Tween and probed with anti-MCL-1 antibody (Cat #600-401-394, Rockland, Gilberstcille, PA) followed by anti-rabbit IgG secondary antibody conjugated to horseradish peroxidase (Southern Biotech, Birmingham, AL). Blots were developed with Immobilon chemiluminescent substrate (Merck Millipore) and images were captured using a BioRad Chemidoc gel imaging system.

Statistics. GraphPad Prism 7.0 software was used for statistical analysis. Statistical comparisons between two groups were made using the Welsh t-test. Statistical comparisons

between multiple groups were made using one-way ANOVA with a Tukey's post hoc test for multiple comparisons. Survival comparisons of mouse genotypes were calculated using the log-ranked (Mantel-Cox) analysis. Differences were considered significant where the p value fell below 0.05 and were classified as follows: *P<0.05, **P<0.01, ***P<0.005, ****P<0.001, P>0.05 ns (not significant).

ACKNOWLEDGEMENTS:

We thank A. Rudensky, B. Kile and P. Bouillet for provision of mice and D. Huang, J. Gong and A. Kallies for other reagents. We are grateful to the WEHI Flow Cytometry Laboratory and Bioservices staff for technical support (particularly H. Marks and G. Siciliano for mouse husbandry) and B. Helbert, C Young and K. Mackwell for genotyping. This work was supported by National Health and Medical Research Council Australia (Grants or Fellowships 1089072 to C.E.T, 1116936 to M.A.F. and 1078763, 1090236, 1145888 and 1158024 to D.H.D.G.), Fellowships by Swiss National Science Foundation and Novartis Foundation for Medical-Biological Research to S.S.G. This research was made possible by grants from the Victorian State Government Operational Infrastructure Support and the Independent Research Institutes Infrastructure Support Scheme of the Australian Government National Health and Medical Research Council.

CONFLICT OF INTEREST STATEMENTS:

Researchers at the Walter and Eliza Hall Institute of Medical Research in the Strasser and Gray laboratories collaborate with Servier on the development of MCL-1 inhibitors.

All other authors declare no competing financial interests.

FIGURE LEGENDS

Figure 1: Abrogation of BAK and BAX rescues the lethal autoinflammatory phenotype of *Mcl1*$^{\Delta FoxP3}$ mice

(**A**) Representative flow cytometry histograms and (**B**) quantification of mean fluorescence intensity of MCL-1 expression in splenic CD4+ T cells from *Mcl1*$^{\Delta FoxP3}$*Bak*$^{-/-}$ mice detected by intracellular flow cytometry in CD4 T conv (CD4$^+$ FOXP3$^-$) and Treg cells (CD4$^+$ FOXP3$^+$). (**C**) Survival curve from birth to 125 days for wild-type, *Mcl1*$^{\Delta FoxP3}$, *Bax*$^{\Delta FoxP3}$*Bak*$^{-/-}$, *Mcl1*$^{\Delta FoxP3}$*Bax*$^{\Delta FoxP3}$*Bak*$^{-/-}$ and *Mcl1*$^{\Delta FoxP3}$*Bak*$^{-/-}$ mice. P-value <0.001 calculated by Log-ranked (Mantel-Cox) test. (**D**) Plasma IgE concentrations in 42-125 day old *Mcl1*$^{\Delta FoxP3}$ mice (taken at time of death or euthanasia) and 125 day old wild-type, *Bak*$^{-/-}$*Bax*$^{\Delta FoxP3}$ and *Mcl1*$^{\Delta FoxP3}$*Bak*$^{-/-}$ *Bax*$^{\Delta FoxP3}$ counterparts. (**E**) Representation of hematoxylin and eosin stained sections of lung, pancreas and salivary gland from 42-125 day old *Mcl1*$^{\Delta FoxP3}$ mice (taken at time of death or euthanasia) and 125 day old wild-type, *Bak*$^{-/-}$*Bax*$^{\Delta FoxP3}$ and *Mcl1*$^{\Delta FoxP3}$*Bak*$^{-/-}$*Bax*$^{\Delta FoxP3}$ counterparts (Scale bar:100 μm). Arrows indicate areas of lymphocytic infiltration. (**F**) Graph of lymphocytic infiltration score in the lung, salivary gland, and pancreas in mice of the indicated genotypes. A higher lymphocytic infiltration score denotes more severe infiltration and organ destruction. Data in (**A**) and (**B**) is representative of 2 independent experiments of 3-4 mice per experiment. Data in (**B**) is mean ± s.d. ****P=0.0003 based on Welch's t test. Data in (**D**) and (**F**) are mean ± s.d. for 7-10 mice per genotype. *P<0.05, **P<0.01, ***P<0.005, ****P<0.001 based on Tukey's multiple comparison test.

Figure 2: Concomitant loss of BAK and BAX prevents the depletion of Treg cells caused by the deletion of MCL-1

(**A**) Representative flow cytometry plots, and (**B**) percentages from total CD4 cells (left) and absolute numbers (right) of CD4$^+$FOXP3$^+$ cells in the thymus of 42-125 day old *Mcl1*$^{\Delta FoxP3}$

mice (taken at time of death or euthanasia) and 125 day old wild-type, *Bak*$^{-/-}$*Bax*$^{\Delta FoxP3}$ and *Mcl1*$^{\Delta FoxP3}$*Bak*$^{-/-}$*Bax*$^{\Delta FoxP3}$ counterparts. (**C**) Representative flow cytometry plots, and (**D**) percentages from total CD4 cells (left) and absolute numbers (right) of CD4^{+}CD25^{+}FOXP3^{+} cells in the spleen and lymph nodes of 42-125 day old *Mcl1*$^{\Delta FoxP3}$ mice (taken at time of severe illness or sacrifice for healthy controls) and 125 day old wild-type, *Bak*$^{-/-}$*Bax*$^{\Delta FoxP3}$ and *Mcl1*$^{\Delta FoxP3}$*Bak*$^{-/-}$*Bax*$^{\Delta FoxP3}$ counterparts. Data in (**A**) and (**C**) are representative of four independent experiments with 1-5 mice in each group. Numbers indicate percentages of cells within the gate. Data in (**B**) and (**D**) represent mean ± s.d. for 8-20 mice per genotype. *P<0.05, **P<0.01, ***P<0.005, ****P<0.001 based on Tukey's multiple comparison test.

Figure 3: The lethal lymphocytic infiltrative disease observed in *Mcl1*$^{\Delta FoxP3}$ mice is a consequence of a constitutively activated immune state.

(**A**) Representative flow cytometry plots of CD44 and CD62L expression on CD4^{+}FOXP3^{-} and CD8^{+} cells from the spleens of 42-125 day old *Mcl1*$^{\Delta FoxP3}$ mice (taken at time of severe illness or sacrifice in the case of healthy controls) and 125 day old wild-type, *Bax*$^{\Delta FoxP3}$*Bak*$^{-/-}$ and *Mcl1*$^{\Delta FoxP3}$*Bax*$^{\Delta FoxP3}$*Bak*$^{-/-}$ counterparts. Numbers indicate percentages of cells in each quadrant. Data in (**A**) are representative of four independent experiments with 1-5 mice in each group. (**B**) Percentages from total CD4 or CD8 cells (left) and absolute numbers (right) of activated CD62L^{low}CD44^{hi} CD4 and CD8 cells in mice of the indicated genotype. Data represent mean ± s.d. for 8-20 mice per genotype. *P<0.05, **P<0.01, ***P<0.005, ****P<0.001 based on Tukey's multiple comparison test.

Figure 4: MCL-1 deficient Treg cells do not have altered metabolic capacity.

(**A**) Representative mitochondrial membrane potential in wild-type, *Mcl1*$^{\Delta FoxP3}$, *Bax*$^{\Delta FoxP3}$*Bak*$^{-/-}$ and *Mcl1*$^{\Delta FoxP3}$*Bax* $^{\Delta FoxP3}$*Bak*$^{-/-}$ Treg cells (TCRβ^{+} CD4^{+} FOXP3^{+} lymphocytes), measured as

accumulation of MitoTracker Orange dye. Representative traces (**B**), and calculated basal (**C**) and maximal (**D**) Oxygen Consumption Rate (OCR) measurements performed on sorted YFP^{+}CD4^{+}CD25^{+} cells from wild type, *Bax*$^{\Delta FoxP3}$*Bak*$^{-/-}$ and *Mcl1*$^{\Delta FoxP3}$*Bax*$^{\Delta FoxP3}$*Bak*$^{-/-}$ mice at basal levels and after subsequent additions of the ATP synthase inhibitor oligomycin, uncoupler FCCP, RC complex I inhibitor rotenone and RC complex III inhibitor antimycin A (AA). Representative traces (**E**), and calculated basal (**F**) and maximal (**G**) OCR and measurements performed on sorted YFP^{+}CD4^{+}CD25^{+} cells from *Bak*$^{-/-}$ chimeric mice treated with DMSO (vehicle), 0.1 μM or 1 μM MCL-1 inhibitor S63845 at basal levels, and after subsequent additions of the oligomycin, FCCP, rotenone and antimycin A. Data in (**A**) are representative of three independent experiments with n=2-5 mice per group. Data in (**B-D**) are mean ± s.d. are representative of three independent experiments. In each experiment, technical replicate wells of 600,000 cells pooled from *n*=2-5 mice were assessed. Data in (**E**) are a representative graph from one experiment of two independent experiments. Data in (**F**) and (**G**) are mean ± s.d. of data pooled from two independent experiments.

Supplementary Figure 1: *Bax*$^{\Delta FoxP3}$*Bak*$^{-/-}$ Treg cells express the OMM and IMM MCL-1 isoforms and have comparable suppressive ability to wild type cells.

(**A**) Quantification of undivided Tconv cells from an *in vitro* Treg cell suppression assay at various ratios of CD4^{+}CD25^{+}YFP^{+} cells:CD4^{+}CD25^{-} Tconv cells from WT control or *Bax*$^{\Delta FoxP3}$*Bak*$^{-/-}$ mice. Data is the average of triplicate measurements and representative of 3 independent experiments. (B) Western blot detection of OMM (~40kDa) and IMM (~31kDa) MCL-1 isoforms in CD4^{+} conventional and regulatory T cells *Bax*$^{\Delta FoxP3}$*Bak*$^{-/-}$.

Supplementary Figure 2: MCL-1 deficient Treg cells do not have altered metabolic capacity.

Calculated basal (**A, C**) and maximal **(B, D**) Oxygen Consumption Rate (OCR) measurements performed on sorted $YFP^{+}CD4^{+}CD25^{+}$ cells from $Bax^{\Delta FoxP3}Bak^{-/-}$ and $Mcl1^{\Delta FoxP3}Bax^{\Delta FoxP3}Bak^{-/-}$ mice at basal levels and after subsequent additions of oligomycin, FCCP, rotenone and antimycin A (AA). Data represent mean ± s.d. for replicate wells within one experiment and in combination with data from three independent experiments.

Supplementary Figure 3: S63845-induced killing of Treg cells is rescued by Bak and Bax deletion.

Cell viability, normalised to vehicle treated control cells, of $CD4^{+}FOXP3^{+}$ Treg cells isolated from wild-type, $Bak^{-/-}$ and $Bax^{\Delta FoxP3}Bak^{-/-}$ mice, treated *in vitro* for 48 h with 0.1 µM, 1 µM or 10µM of S63845. Data in are mean ± s.d. for two independent experiments.

REFERENCES

1. Strasser A, O'Connor L, Dixit VM. Apoptosis signaling. *Annu Rev Biochem* 2000, **69:** 217-245.

2. Delbridge AR, Strasser A. The BCL-2 protein family, BH3-mimetics and cancer therapy. *Cell Death Differ* 2015, **22**(7)**:** 1071-1080.

3. Meier P, Finch A, Evan G. Apoptosis in development. *Nature* 2000, **407**(6805)**:** 796-801.

4. Vo TT, Letai A. BH3-only proteins and their effects on cancer. *Adv Exp Med Biol* 2010, **687:** 49-63.

5. Doerflinger M, Glab JA, Puthalakath H. BH3-only proteins: a 20-year stock-take. *FEBS J* 2015, **282**(6)**:** 1006-1016.

6. Adams JM, Cory S. The BCL-2 arbiters of apoptosis and their growing role as cancer targets. *Cell Death Differ* 2018, **25**(1)**:** 27-36.

7. Josefowicz SZ, Lu LF, Rudensky AY. Regulatory T cells: mechanisms of differentiation and function. *Annu Rev Immunol* 2012, **30:** 531-564.

8. Fontenot JD, Gavin MA, Rudensky AY. Foxp3 programs the development and function of CD4+CD25+ regulatory T cells. *Nat Immunol* 2003, **4**(4)**:** 330-336.

9. Sakaguchi S, Sakaguchi N, Asano M, Itoh M, Toda M. Immunologic self-tolerance maintained by activated T cells expressing IL-2 receptor alpha-chains (CD25). Breakdown of a single mechanism of self-tolerance causes various autoimmune diseases. *J Immunol* 1995, **155**(3)**:** 1151-1164.

10. Liston A, Gray DH. Homeostatic control of regulatory T cell diversity. *Nat Rev Immunol* 2014, **14**(3)**:** 154-165.

11. Bennett CL, Christie J, Ramsdell F, Brunkow ME, Ferguson PJ, Whitesell L*, et al.* The immune dysregulation, polyendocrinopathy, enteropathy, X-linked syndrome (IPEX) is caused by mutations of FOXP3. *Nat Genet* 2001, **27**(1)**:** 20-21.

12. Bennett CL, Ochs HD. IPEX is a unique X-linked syndrome characterized by immune dysfunction, polyendocrinopathy, enteropathy, and a variety of autoimmune phenomena. *Curr Opin Pediatr* 2001, **13**(6)**:** 533-538.

13. Wildin RS, Ramsdell F, Peake J, Faravelli F, Casanova JL, Buist N*, et al.* X-linked neonatal diabetes mellitus, enteropathy and endocrinopathy syndrome is the human equivalent of mouse scurfy. *Nat Genet* 2001, **27**(1)**:** 18-20.

14. Hori S, Nomura T, Sakaguchi S. Control of regulatory T cell development by the transcription factor Foxp3. *Science* 2003, **299**(5609)**:** 1057-1061.

15. Khattri R, Cox T, Yasayko SA, Ramsdell F. An essential role for Scurfin in CD4+CD25+ T regulatory cells. *Nat Immunol* 2003, **4**(4)**:** 337-342.

16. Attias M, Al-Aubodah T, Piccirillo CA. Mechanisms of human FoxP3(+) Treg cell development and function in health and disease. *Clin Exp Immunol* 2019, **197**(1)**:** 36-51.

17. Mathis D. Immunological goings-on in visceral adipose tissue. *Cell Metab* 2013, **17**(6)**:** 851-859.

18. Passerini L, Bacchetta R. Forkhead-Box-P3 Gene Transfer in Human CD4(+) T Conventional Cells for the Generation of Stable and Efficient Regulatory T Cells, Suitable for Immune Modulatory Therapy. *Front Immunol* 2017, **8:** 1282.

19. Perdigoto AL, Chatenoud L, Bluestone JA, Herold KC. Inducing and Administering Tregs to Treat Human Disease. *Front Immunol* 2015, **6:** 654.

20. Zhang D, Tu E, Kasagi S, Zanvit P, Chen Q, Chen W. Manipulating regulatory T cells: a promising strategy to treat autoimmunity. *Immunotherapy* 2015, **7**(11)**:** 1201-1211.

21. Passerini L, Rossi Mel E, Sartirana C, Fousteri G, Bondanza A, Naldini L*, et al.* CD4(+) T cells from IPEX patients convert into functional and stable regulatory T cells by FOXP3 gene transfer. *Sci Transl Med* 2013, **5**(215)**:** 215ra174.

22. Pierson W, Cauwe B, Policheni A, Schlenner SM, Franckaert D, Berges J*, et al.* Antiapoptotic Mcl-1 is critical for the survival and niche-filling capacity of Foxp3(+) regulatory T cells. *Nat Immunol* 2013, **14**(9)**:** 959-965.

23. Carrington EM, Zhan Y, Brady JL, Zhang JG, Sutherland RM, Anstee NS*, et al.* Anti-apoptotic proteins BCL-2, MCL-1 and A1 summate collectively to maintain survival of immune cell populations both in vitro and in vivo. *Cell Death Differ* 2017, **24**(5)**:** 878-888.

24. Kotschy A, Szlavik Z, Murray J, Davidson J, Maragno AL, Le Toumelin-Braizat G*, et al.* The MCL1 inhibitor S63845 is tolerable and effective in diverse cancer models. *Nature* 2016, **538**(7626)**:** 477-482.

25. Merino D, Whittle JR, Vaillant F, Serrano A, Gong JN, Giner G*, et al.* Synergistic action of the MCL-1 inhibitor S63845 with current therapies in preclinical models of triple-negative and HER2-amplified breast cancer. *Sci Transl Med* 2017, **9**(401).

26. Weeden CE, Ah-Cann C, Holik AZ, Pasquet J, Garnier JM, Merino D*, et al.* Dual inhibition of BCL-XL and MCL-1 is required to induce tumour regression in lung squamous cell carcinomas sensitive to FGFR inhibition. *Oncogene* 2018, **37**(32)**:** 4475-4488.

27. Brennan MS, Chang C, Tai L, Lessene G, Strasser A, Dewson G*, et al.* Humanized Mcl-1 mice enable accurate preclinical evaluation of MCL-1 inhibitors destined for clinical use. *Blood* 2018, **132**(15)**:** 1573-1583.

28. Caenepeel S, Brown SP, Belmontes B, Moody G, Keegan KS, Chui D*, et al.* AMG 176, a Selective MCL1 Inhibitor, Is Effective in Hematologic Cancer Models Alone and in Combination with Established Therapies. *Cancer Discov* 2018, **8**(12)**:** 1582-1597.

29. Perciavalle RM, Stewart DP, Koss B, Lynch J, Milasta S, Bathina M*, et al.* Anti-apoptotic MCL-1 localizes to the mitochondrial matrix and couples mitochondrial fusion to respiration. *Nat Cell Biol* 2012, **14**(6)**:** 575-583.

30. Wang X, Bathina M, Lynch J, Koss B, Calabrese C, Frase S*, et al.* Deletion of MCL-1 causes lethal cardiac failure and mitochondrial dysfunction. *Genes Dev* 2013, **27**(12)**:** 1351-1364.

31. Rasmussen ML, Kline LA, Park KP, Ortolano NA, Romero-Morales AI, Anthony CC*, et al.* A Non-apoptotic Function of MCL-1 in Promoting Pluripotency and Modulating Mitochondrial Dynamics in Stem Cells. *Stem Cell Reports* 2018, **10**(3)**:** 684-692.

32. Rasmussen ML, Taneja N, Neininger AC, Wang L, Robertson GL, Riffle SN*, et al.* MCL-1 Inhibition by Selective BH3 Mimetics Disrupts Mitochondrial Dynamics Causing Loss of Viability and Functionality of Human Cardiomyocytes. *iScience* 2020, **23**(4)**:** 101015.

33. Zeng H, Yang K, Cloer C, Neale G, Vogel P, Chi H. mTORC1 couples immune signals and metabolic programming to establish T(reg)-cell function. *Nature* 2013, **499**(7459)**:** 485-490.

34. Vikstrom I, Carotta S, Luthje K, Peperzak V, Jost PJ, Glaser S*, et al.* Mcl-1 is essential for germinal center formation and B cell memory. *Science* 2010, **330**(6007)**:** 1095-1099.

35. Rubtsov YP, Rasmussen JP, Chi EY, Fontenot J, Castelli L, Ye X*, et al.* Regulatory T cell-derived interleukin-10 limits inflammation at environmental interfaces. *Immunity* 2008, **28**(4)**:** 546-558.

36. Godfrey VL, Wilkinson JE, Rinchik EM, Russell LB. Fatal lymphoreticular disease in the scurfy (sf) mouse requires T cells that mature in a sf thymic environment: potential model for thymic education. *Proc Natl Acad Sci U S A* 1991, **88**(13)**:** 5528-5532.

37. Godfrey VL, Wilkinson JE, Russell LB. X-linked lymphoreticular disease in the scurfy (sf) mutant mouse. *Am J Pathol* 1991, **138**(6)**:** 1379-1387.

38. Takeuchi O, Fisher J, Suh H, Harada H, Malynn BA, Korsmeyer SJ. Essential role of BAX,BAK in B cell homeostasis and prevention of autoimmune disease. *Proc Natl Acad Sci U S A* 2005, **102**(32)**:** 11272-11277.

39. Willis SN, Chen L, Dewson G, Wei A, Naik E, Fletcher JI*, et al.* Proapoptotic Bak is sequestered by Mcl-1 and Bcl-xL, but not Bcl-2, until displaced by BH3-only proteins. *Genes Dev* 2005, **19**(11)**:** 1294-1305.

40. Zhai D, Jin C, Huang Z, Satterthwait AC, Reed JC. Differential regulation of Bax and Bak by anti-apoptotic Bcl-2 family proteins Bcl-B and Mcl-1. *J Biol Chem* 2008, **283**(15)**:** 9580-9586.

41. Wali JA, Galic S, Tan CY, Gurzov EN, Frazier AE, Connor T*, et al.* Loss of BIM increases mitochondrial oxygen consumption and lipid oxidation, reduces adiposity and improves insulin sensitivity in mice. *Cell Death Differ* 2018, **25**(1)**:** 217-225.

42. Tripathi P, Koss B, Opferman JT, Hildeman DA. Mcl-1 antagonizes Bax/Bak to promote effector CD4(+) and CD8(+) T-cell responses. *Cell Death Differ* 2013, **20**(8)**:** 998-1007.

43. Beier UH, Angelin A, Akimova T, Wang L, Liu Y, Xiao H*, et al.* Essential role of mitochondrial energy metabolism in Foxp3(+) T-regulatory cell function and allograft survival. *FASEB J* 2015, **29**(6)**:** 2315-2326.

44. Howie D, Cobbold SP, Adams E, Ten Bokum A, Necula AS, Zhang W*, et al.* Foxp3 drives oxidative phosphorylation and protection from lipotoxicity. *JCI Insight* 2017, **2**(3)**:** e89160.

45. Chen YB, Aon MA, Hsu YT, Soane L, Teng X, McCaffery JM*, et al.* Bcl-xL regulates mitochondrial energetics by stabilizing the inner membrane potential. *J Cell Biol* 2011, **195**(2)**:** 263-276.

46. Angelin A, Gil-de-Gomez L, Dahiya S, Jiao J, Guo L, Levine MH*, et al.* Foxp3 Reprograms T Cell Metabolism to Function in Low-Glucose, High-Lactate Environments. *Cell Metab* 2017, **25**(6)**:** 1282-1293 e1287.

47. Galgani M, De Rosa V, La Cava A, Matarese G. Role of Metabolism in the Immunobiology of Regulatory T Cells. *J Immunol* 2016, **197**(7)**:** 2567-2575.

48. Clambey ET, McNamee EN, Westrich JA, Glover LE, Campbell EL, Jedlicka P*, et al.* Hypoxia-inducible factor-1 alpha-dependent induction of FoxP3 drives regulatory T-cell abundance and function during inflammatory hypoxia of the mucosa. *Proc Natl Acad Sci U S A* 2012, **109**(41)**:** E2784-2793.

49. Dang EV, Barbi J, Yang HY, Jinasena D, Yu H, Zheng Y*, et al.* Control of T(H)17/T(reg) balance by hypoxia-inducible factor 1. *Cell* 2011, **146**(5)**:** 772-784.

50. Shi LZ, Wang R, Huang G, Vogel P, Neale G, Green DR*, et al.* HIF1alpha-dependent glycolytic pathway orchestrates a metabolic checkpoint for the differentiation of TH17 and Treg cells. *J Exp Med* 2011, **208**(7)**:** 1367-1376.

51. Teh CE, Daley SR, Enders A, Goodnow CC. T-cell regulation by casitas B-lineage lymphoma (Cblb) is a critical failsafe against autoimmune disease due to autoimmune regulator (Aire) deficiency. *Proc Natl Acad Sci U S A* 2010, **107**(33)**:** 14709-14714.

676
677

Figure 1

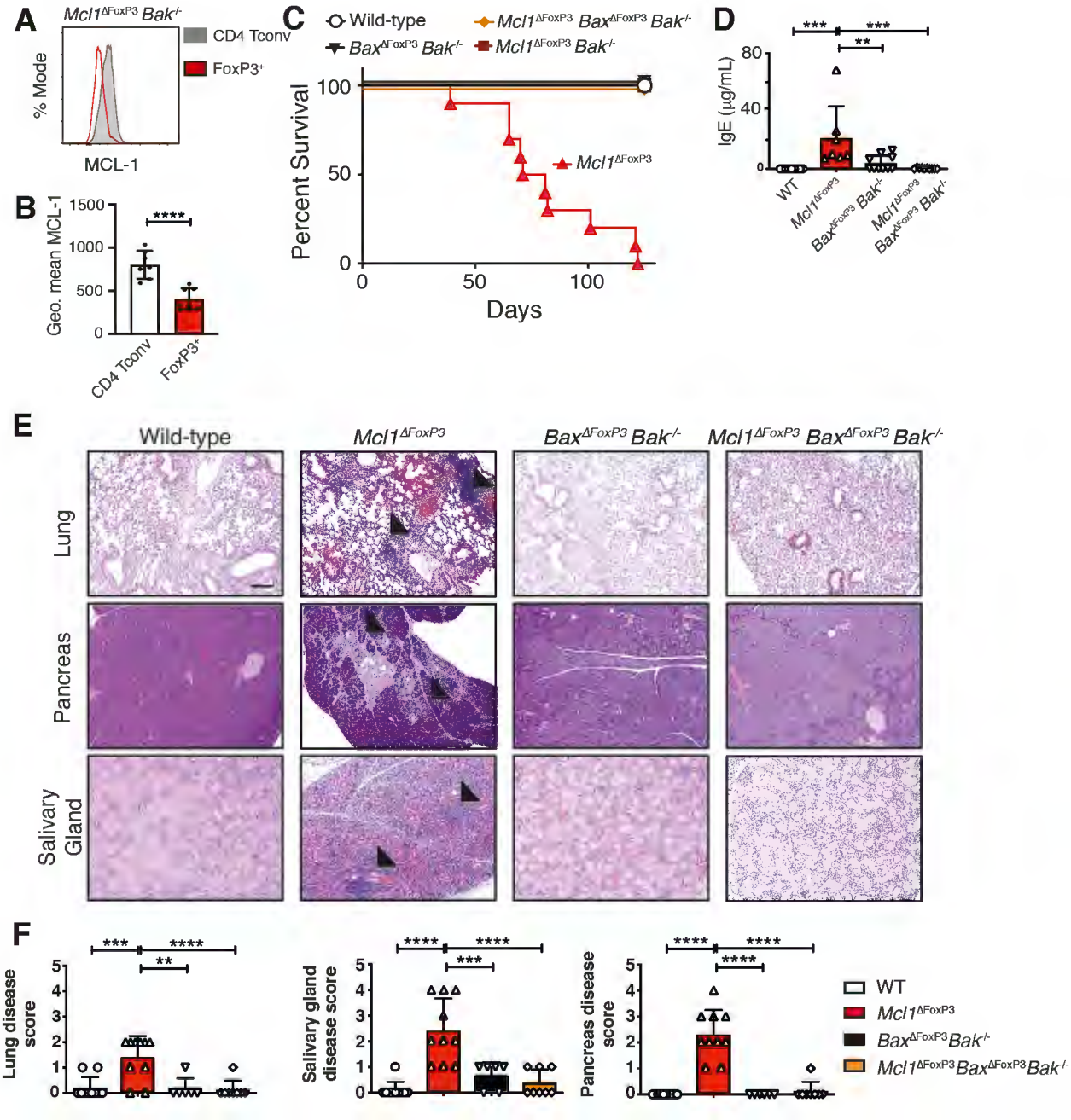
A
Mcl1ΔFoxP3 Bak-/-
CD4 Tconv
FoxP3+
% Mode
MCL-1
B
Geo. mean MCL-1
1500
1000
500
0
****
CD4 Tconv
FoxP3+
C
Wild-type
Mcl1ΔFoxP3 BaxΔFoxP3 Bak-/-
BaxΔFoxP3 Bak-/-
Mcl1ΔFoxP3 Bak-/-
Percent Survival
100
50
0
Mcl1ΔFoxP3
0
50
100
Days
D
***
***
**
IgE (μg/mL)
80
40
0
WT
Mcl1ΔFoxP3
BaxΔFoxP3 Bak-/-
Mcl1ΔFoxP3 BaxΔFoxP3 Bak-/-
E
Wild-type
Mcl1ΔFoxP3
BaxΔFoxP3 Bak-/-
Mcl1ΔFoxP3 BaxΔFoxP3 Bak-/-
Lung
Pancreas
Salivary Gland
F
Lung disease score
Salivary gland disease score
Pancreas disease score
WT
Mcl1ΔFoxP3
BaxΔFoxP3Bak-/-
Mcl1ΔFoxP3BaxΔFoxP3Bak-/-

Figure 2

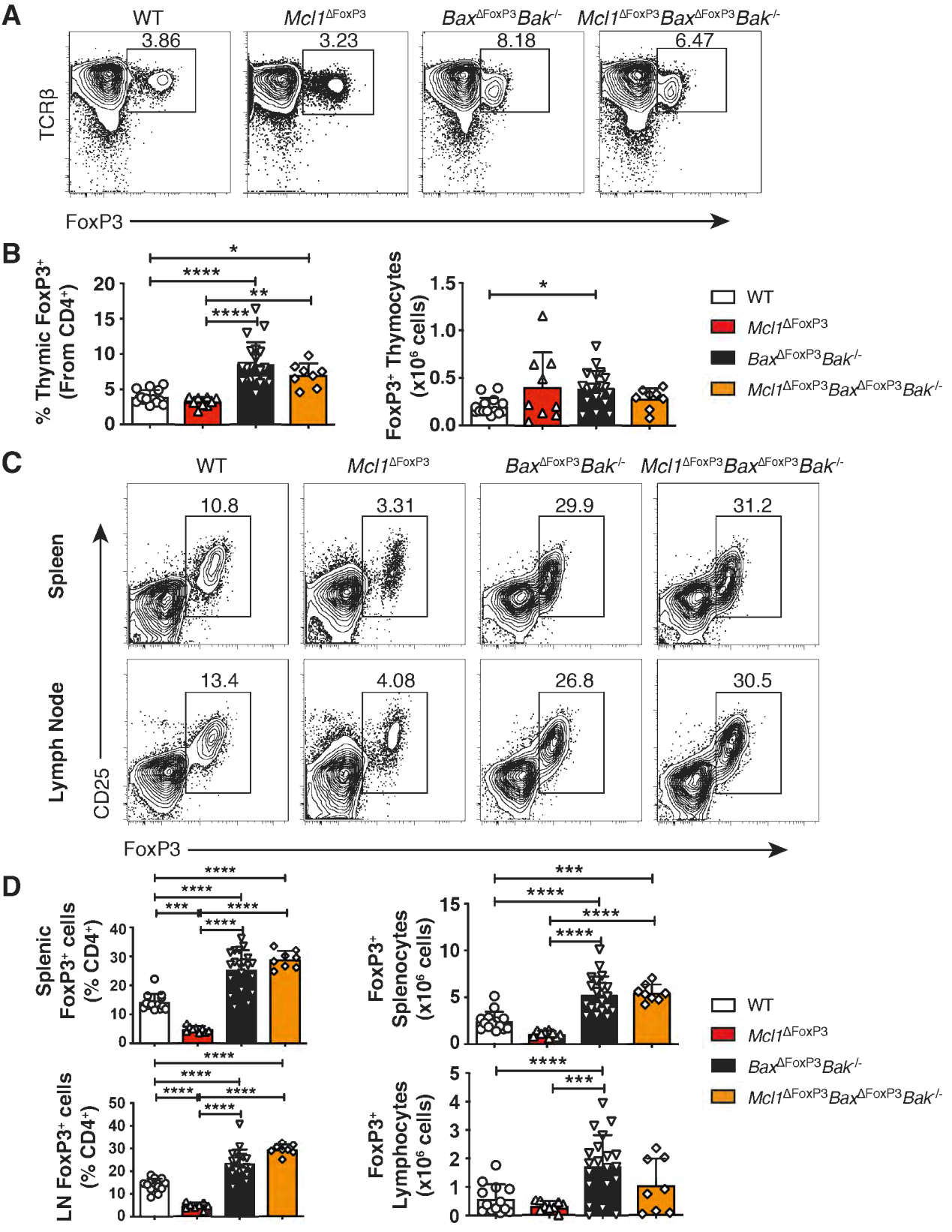
A
WT
Mcl1ΔFoxP3
BaxΔFoxP3Bak-/-
Mcl1ΔFoxP3BaxΔFoxP3Bak-/-
3.86
3.23
8.18
6.47
TCRβ
FoxP3
B
% Thymic FoxP3+ (From CD4+)
FoxP3+ Thymocytes (x10^6 cells)
WT
Mcl1ΔFoxP3
BaxΔFoxP3Bak-/-
Mcl1ΔFoxP3BaxΔFoxP3Bak-/-
C
WT
Mcl1ΔFoxP3
BaxΔFoxP3Bak-/-
Mcl1ΔFoxP3BaxΔFoxP3Bak-/-
Spleen
Lymph Node
10.8
3.31
29.9
31.2
13.4
4.08
26.8
30.5
CD25
FoxP3
D
Splenic FoxP3+ cells (% CD4+)
LN FoxP3+ cells (% CD4+)
FoxP3+ Splenocytes (x10^6 cells)
FoxP3+ Lymphocytes (x10^6 cells)
WT
Mcl1ΔFoxP3
BaxΔFoxP3Bak-/-
Mcl1ΔFoxP3BaxΔFoxP3Bak-/-

Figure 3

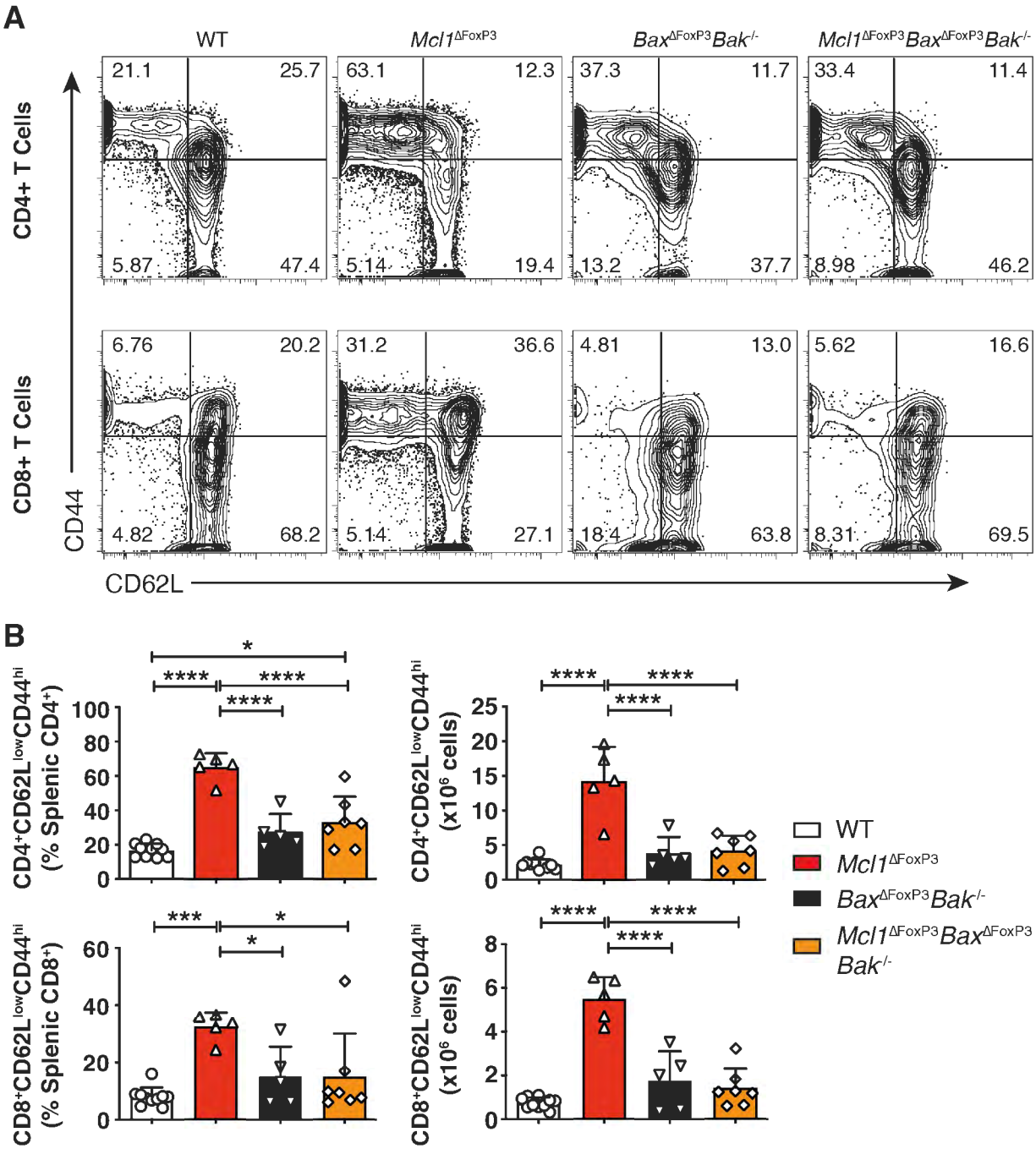
A
WT
Mcl1ΔFoxP3
BaxΔFoxP3Bak-/-
Mcl1ΔFoxP3BaxΔFoxP3Bak-/-
CD4+ T Cells
CD8+ T Cells
CD44
CD62L
21.1
25.7
5.87
47.4
63.1
12.3
5.14
19.4
37.3
11.7
13.2
37.7
33.4
11.4
8.98
46.2
6.76
20.2
4.82
68.2
31.2
36.6
5.14
27.1
4.81
13.0
18.4
63.8
5.62
16.6
8.31
69.5
B
CD4+CD62Llow CD44hi (% Splenic CD4+)
CD4+CD62Llow CD44hi (x10^6 cells)
CD8+CD62Llow CD44hi (% Splenic CD8+)
CD8+CD62Llow CD44hi (x10^6 cells)
WT
Mcl1ΔFoxP3
BaxΔFoxP3Bak-/-
Mcl1ΔFoxP3BaxΔFoxP3 Bak-/-

Figure 4

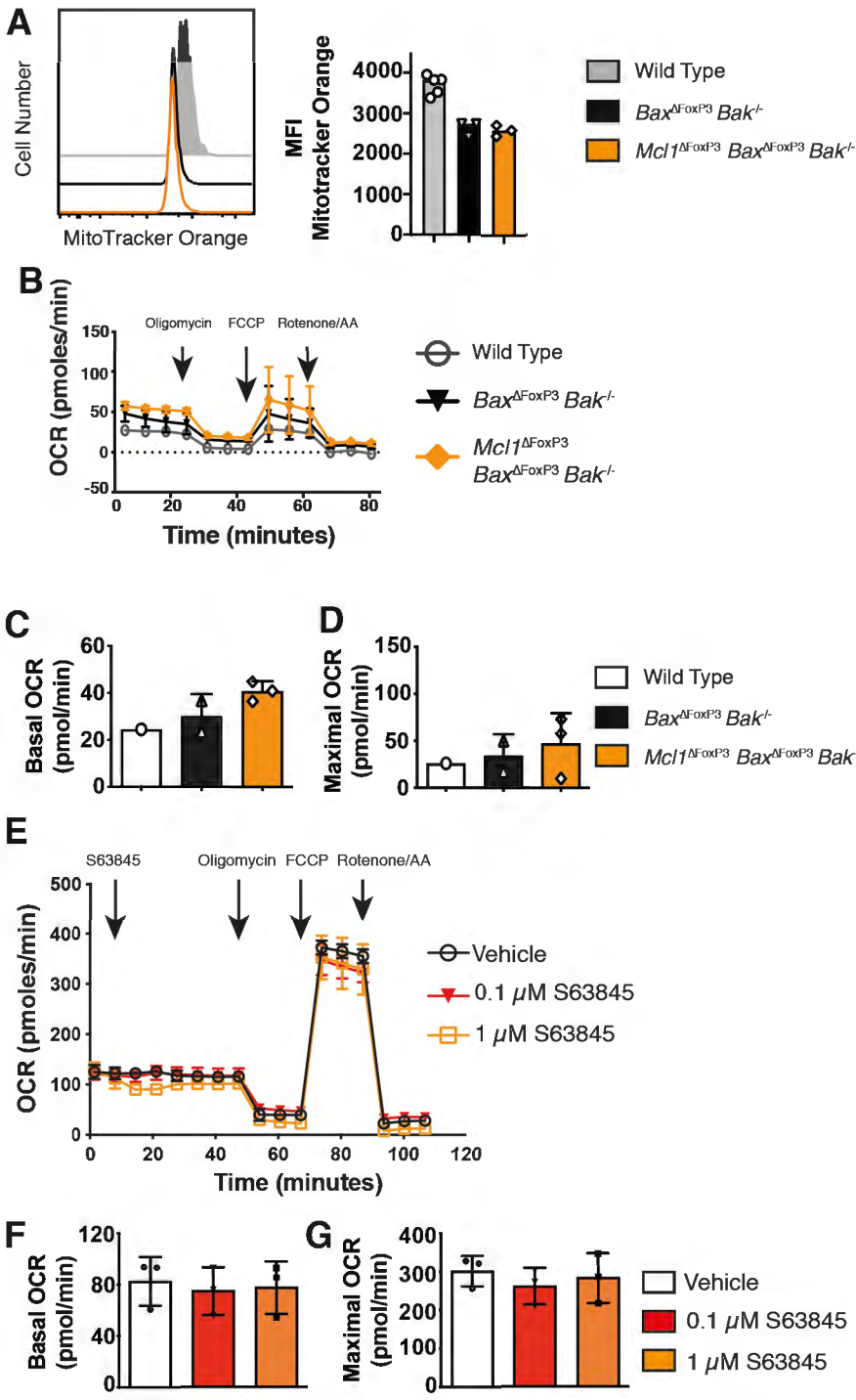
A
Cell Number
MitoTracker Orange
MFI Mitotracker Orange
4000
3000
2000
1000
0
Wild Type
Bax^ΔFoxP3 Bak^-/-
Mcl1^ΔFoxP3 Bax^ΔFoxP3 Bak^-/-
B
Oligomycin
FCCP
Rotenone/AA
OCR (pmoles/min)
150
100
50
0
-50
0
20
40
60
80
Time (minutes)
Wild Type
Bax^ΔFoxP3 Bak^-/-
Mcl1^ΔFoxP3 Bax^ΔFoxP3 Bak^-/-
C
Basal OCR (pmol/min)
60
40
20
0
D
Maximal OCR (pmol/min)
150
100
50
0
Wild Type
Bax^ΔFoxP3 Bak^-/-
Mcl1^ΔFoxP3 Bax^ΔFoxP3 Bak^-/-
E
S63845
Oligomycin
FCCP
Rotenone/AA
OCR (pmoles/min)
500
400
300
200
100
0
0
20
40
60
80
100
120
Time (minutes)
Vehicle
0.1 μM S63845
1 μM S63845
F
Basal OCR (pmol/min)
120
80
40
0
G
Maximal OCR (pmol/min)
400
300
200
100
0
Vehicle
0.1 μM S63845
1 μM S63845

Supplementary Figure S1

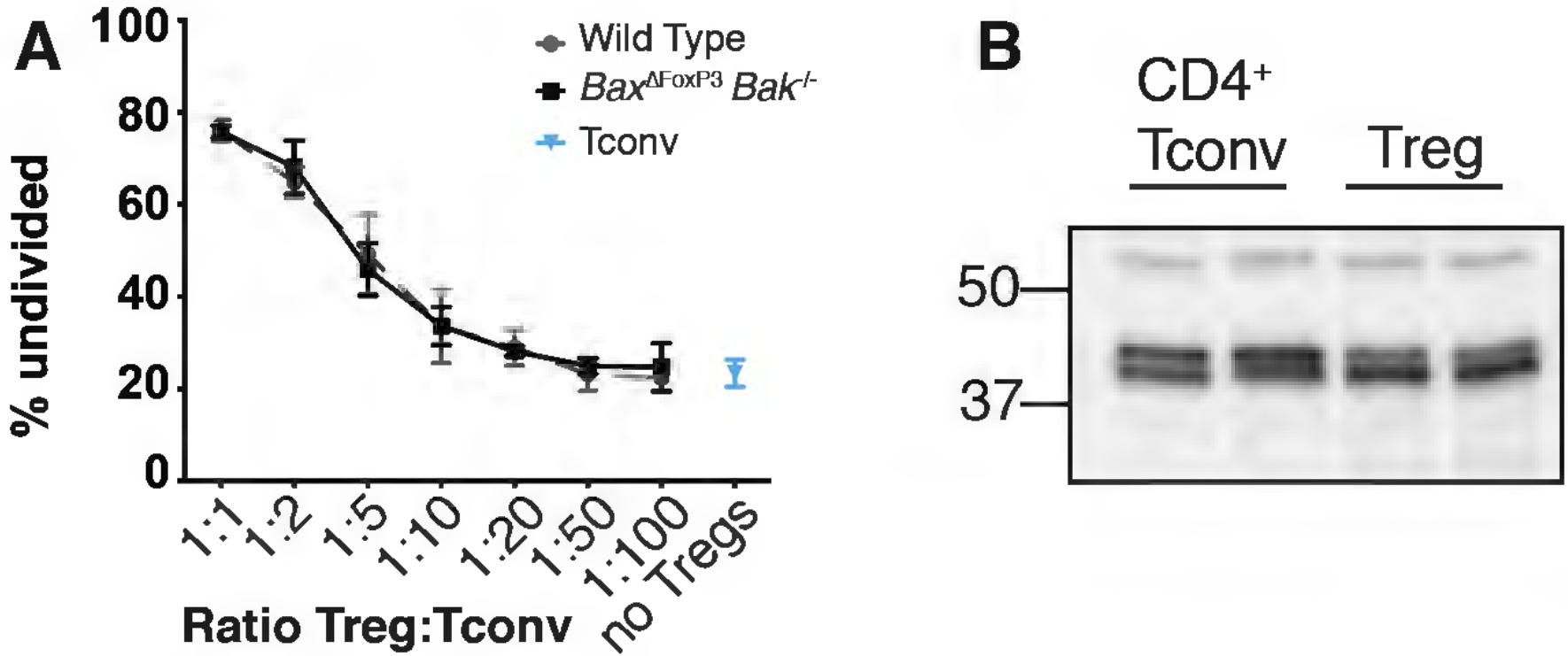

Supplementary Figure S2

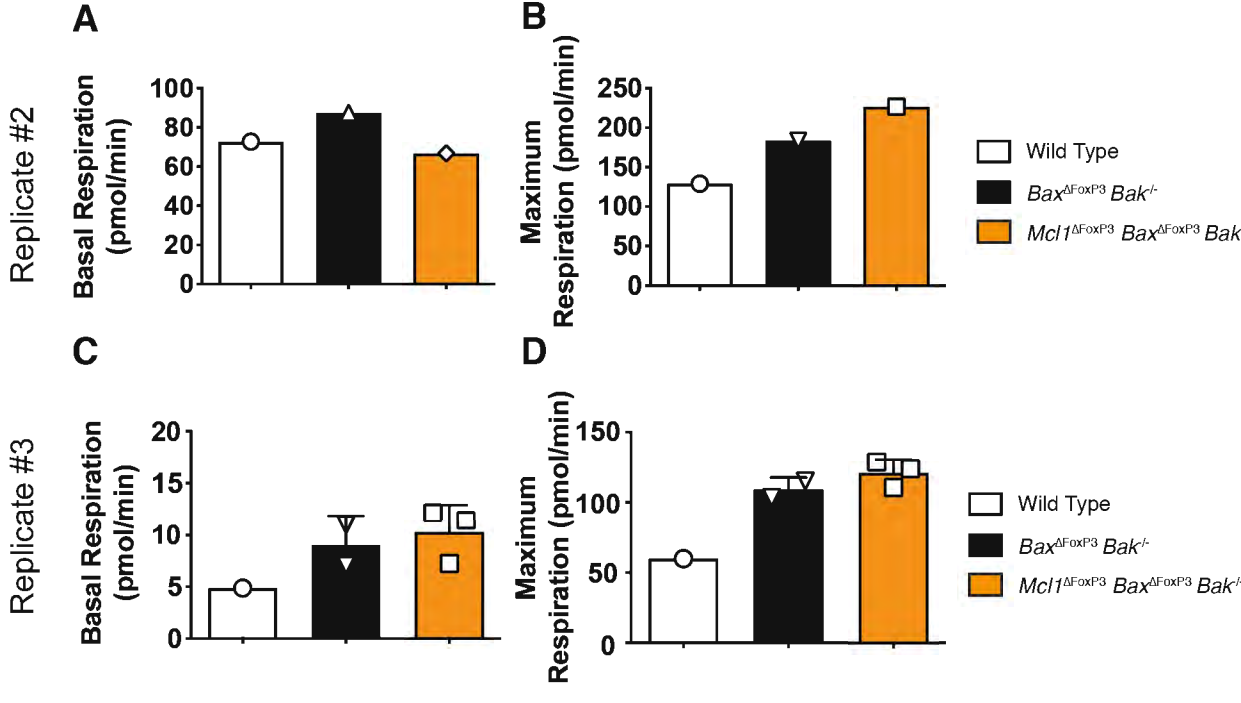

Supplementary Figure S3